MD Calculated Structural Properties of Clusters in Liquid Acetonitrile/Water Mixtures with Various Contents of Acetonitrile

Christian Oldiges,*,† Kai Wittler,† Thorsten Tönsing,† and Alexander Alijah‡

Universität Bielefeld, Fakultät für Chemie, Theoretische Chemie, Postfach 10 01 31, 33 501 Bielefeld, Germany, and Universidade de Coimbra, Departamento de Química, 3004-535 Coimbra, Portugal

Received: January 7, 2002; In Final Form: May 17, 2002

The diversity of the water and acetonitrile structures in a binary system, caused by local structural inhomogeneities, has been investigated by molecular dynamic simulations. Our systems cover a broad range of acetonitrile mole fractions: dilute, moderate, and higher concentration mixtures. For reference, we perform simulations on pure water and pure acetonitrile systems. We examine concepts of analysis for an extraction of local structure information of anisotropic fluids. In general, the local water and acetonitrile structures can be roughly characterized by the radial distribution functions in terms of the classical site−site pair correlations. For a more thorough investigation of the local structure and the microheterogeneity of the systems, we use angular-dependent radial distribution functions. From the radial pair correlation functions, it is possible to extract coordination numbers and detailed local information of anisotropic water distributions around the acetonitrile molecules. To confirm the existence of the acetonitrile cluster and to gain qualitative insight into its stability, we examined the time-dependent radial and angular distribution functions. The results for the acetonitrile cluster arrangements are in line with experimental data of binary acetonitrile/water mixtures.

Introduction

Detailed information on the molecular level of physicochemical properties of a system can be obtained from MD simulations. Investigations of the trajectories of MD simulations by adequate methods of analysis lead to an understanding of the interactions of the molecules and their properties, which correlate well with experimental data.

Binary liquid systems such as acetonitrile (AN)/water mixtures are frequently used in a variety of fields such as organic synthesis, electrochemistry, chromatography, and solvent extraction because certain properties of these mixtures differ from those of conventional organic solvents such as chloroform. Some special characteristics of AN are its aprotic, polar, and organic properties. For example, it is possible under normal conditions to dissolve the organic component AN in water at various mole fractions and also in many other inorganic or organic substances.

Many studies have been published on theoretical, molecular dynamics, and experimental aspects of such systems. From their investigations of the binary system AN/H_2O, Robertson and Sugamori[1] concluded that the AN molecule behaves like a small ion and disrupts the liquid structure of water. However, the thermodynamical studies of Moreau and Douheret[2] and also the Raman spectroscopy studies of von Kabisch[3] show that the AN molecules in the range of 0−20 mol % AN occupy free "cages" in the liquid water structure, so the stability of the water structure does not change significantly. Von Kabisch has shown that for binary systems consisting of more than 20 mol % AN, the water component of the binary system becomes more structured than pure water. According to the Naberukin−Rogov model,[4] a microheterogeneous structure appears in this kind of binary mixture. Microheterogeneity can be understood as the deviation from the average distribution of molecules on a local microscopic level. A mixture, seemingly homogeneous on the macroscopic level, is heterogeneous on the microscopic level. In solution, the AN molecules are not distributed homogeneously; rather, they form various "clusters" within the mixture. Any two volume sectors of a macroscopically homogeneous system that are sufficiently large microscopically but small macroscopically have the same physical properties. Such volume sectors are microhomogeneous if their constituents are, on average, equally distributed throughout their volumes. Consider for example a mixture of point-charged particles such as alkali cations and water in which the water environment around the ions is spherical. Because of this symmetry, the mixture is homogeneous. In an AN/H_2O mixture, however, the nonspherical asymmetric structure of the AN molecule, which on one hand has a spatially extended methyl group and on the other hand, a nitrile group with a highly negative partial charge, leads to microscopic heterogeneity.

Goldammer and Hertz[5] observed an increase in the water structure at low AN concentrations and also found a certain degree of microheterogeneity in AN/water mixtures. Kovacs and Laaksonen[6,7] performed MD simulations on a short time scale (20 ps) on pure water, pure AN, and AN/H_2O mixtures with 12, 50, and 88 mol % AN. They used the single point-charge (SPC) water model[8] and the six-site model of Böhm[9] for the AN molecule. Mountain[10] performed simulations on AN/H_2O mixtures with 10−90 mol % AN in 10 mol % steps using the extended single point-charge (SPC/E) water model[11] and the three-site model for AN, which describes the methyl group only as a point and thus ignores the spatial extension of the methyl hydrogen atoms. On the basis of the conventional radial distribution functions, Kovacs and Laaksonen[6,7] and Mountain[10] found indications for microheterogeneity in those mixtures

* Corresponding author. E-mail: chriso@uni-bielefeld.de.
† Universität Bielefeld.
‡ Universidade de Coimbra.

10.1021/jp025506d CCC: $22.00
Published on Web 07/13/2002

beginning with 12 mol % AN or 10 mol % AN, respectively. By means of the ensemble standardized radial distribution functions, they obtained distance-dependent information but no angular relations, which would be necessary for a more detailed analysis of the structure. With X-ray diffraction and IR spectroscopic methods, Takamuku et al.[12] succeeded in experimentally proving the coexistence of AN and water clusters. Furthermore, they give more detailed structural information, mainly for the AN cluster.

In the Methods section, We introduce the statistical techniques for the angular- and time-dependent pair correlation functions. Then we discuss our results by comparing the results of Kovacs' simulations[6] and Takamuku's experimental data.[12] By means of the introduced methods of analysis, we are able to determine the local microscopic cluster structure of the mixture's compounds.

Simulation Details

For the build up of the binary AN/H_2O system, we first place the nitrile carbon (C1) of the AN molecule randomly in a free region of the cubic box with periodic boundary conditions. Furthermore, the direction of the main axis of this AN is chosen randomly. The nitrogen atom and methyl carbon (C2) are placed along the main axis. The direction and position of the first hydrogen atom are chosen randomly, whereas the N−C2−H1 angle is 110° and the C2−H1 bond length is 1 Å. A subsequent rotation around the top axis defines the positions of the other two hydrogen atoms and completes the AN molecule according to a tetrahedral arrangement at the methyl carbon.[13] This procedure is repeated until the required number of AN molecules is reached. Each AN was generated as a rigid six-site molecule model using Böhm's[14] parameter set. Finally, we place water molecules in the simulation box until the required AN/H_2O value is achieved. These water molecules are generated by Berendsen's SPC/E[11] water model, which treats the water molecule as a rigid three-site model. Once the start configurations are generated, one has to remove the strong internal tension of the unequilibrated systems. During the first equilibration period of the simulations in the NVT ensemble, the Woodcock thermostat,[15] a modified leapfrog algorithm, was used. The integration steps have been increased slowly from 10^{-3} fs at the beginning to 1 fs at the end, depending on the degree of temperature correction. To adjust the selected temperature of 300 K and to escape from local energy minima, a second equilibration phase of 50 ps with 1-fs steps in the NVT ensemble was found to be necessary.

For the simulation runs performed with 1-fs time steps, the simulation time and the corresponding sampling rate are shown in Table 1. For the integration, we apply the velocity Verlet method of Swope et al.[16] In each integration step, the RATTLE[17,18] algorithm was used to relax the initially constrained bonds of the rigid AN molecules and the hydrogen atoms. Then, the temperature was fixed in the NVT ensemble by a Berendsen−Thermostat[19] with a coupling time of 0.5 ps. For the calculation of the Lennard-Jones parameters, the Jorgensen[20] combination rules have been used. The Lennard-Jones interactions were truncated using a cutoff radius of 10 Å. For an accurate calculation of the long-range Coulomb interactions, the Ewald sum technique[16,21−27] was applied with the same cutoff for the real term of the summation.

Methods

Using the radial pair distribution function (RDF), $g_{A-B}(r)$, and the angle-dependent radial pair distribution function,

TABLE 1: Composition of the Simulation Systems

AN[a]	H_2O[a]	mol % AN	density,[b] g/cm^3	time,[c] ps	rate,[d] /fs
0	390	0.00	1.00	100	10
1	385	0.26	1.00	300	20
2	379	0.50	1.00	350	20
4	379	1.00	1.00	350	20
6	364	1.60	1.00	300	20
8	355	2.20	1.00	1000	50
16	322	4.70	1.00	1000	50
24	292	7.60	0.99	500	50
32	243	11.60	0.98	500	50
80	242	24.80	0.91	250	20
160	158	50.30	0.85	200	20
240	79	75.20	0.82	200	20
320	0	100.0	0.78	200	20

[a] Molecules. [b] Of the solution. [c] Run duration. [d] Sampling rate.

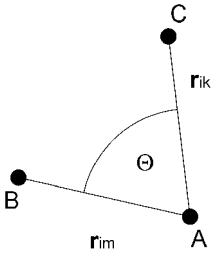

Figure 1. Illustration of the angular and radial relationship between the molecule containing atoms A and B and the correlated atom C, which is used in the angular-dependent RDF $g_{A-B,C}(r, \Theta)$.

$g_{A-B,C}(r, \Theta)$, information about the microscopic structure can be obtained. The conventional RDF is useful for binary systems with dissolved particles, which are spherically symmetric, such as mononuclear ions, in describing the structure of the clusters. However, if the solvated particle, such as the AN molecule, is structured, (i.e., if the solvated molecule consists of different kinds of spatially extended functional groups or different partial charge), then the conventional RDFs still suggest a spherically symmetrical distribution of the correlated particles because these functions relate only to the statistical mean of the distance between two particles. We think that an adequate method for structural analysis has to be based on the angular-dependent pair distribution function.

Because both distance and angle intervals are taken into account,

$$g_{A-B,C}(r, \Theta) = \frac{V_{box}}{tN_A N_C V(r, r+\Delta r, \Theta, \Theta+\Delta\Theta)} \sum_{\tau=1}^{t} \sum_{i=1}^{N_A} \sum_{j=1}^{N_B/N_A} \sum_{k=1}^{N_C} \delta_{\Delta r}(r - |\mathbf{r}_{ik}(\tau)|) \quad (1)$$

$$\delta_{\Delta\Theta}\left(\Theta - \arccos\left(\frac{\mathbf{r}_{im}(\tau)\,\mathbf{r}_{ik}(\tau)}{|\mathbf{r}_{im}(\tau)||\mathbf{r}_{ik}(\tau)|}\right)\right)$$

$$\text{with } m = (i-1)N_B/N_A + j$$

$$\text{and } \delta_{\Delta\Theta}(\Theta) = \begin{cases} 1 & \forall\ 0 \le \Theta \le \Delta\Theta \\ 0 & \text{elsewhere} \end{cases} \quad (2)$$

Θ is the angle between two vectors. The basis vector $\mathbf{r}_{im}$ (see Figure 1) is defined by the positions of the atoms A and B, which belong to the same molecule, whereas A marks the center of the correlation. The second vector $\mathbf{r}_{ik}$ is defined by the positions of the atoms A and C, where C belongs to the correlated (different) molecules and r is the length of the vector

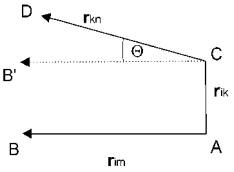

Figure 2. Illustration of the radial and angular relationship between two molecules containing atoms A and B or C and D, which is used in the angular-dependent RDF $g_{A-B,C-D}(r, \Theta)$.

represented by atoms A and C. V_{box} is the volume of the simulation box; t is the simulation time; N_A, N_B, and N_C are the numbers of the atoms A, B, or C, respectively. The volume of the spherical sector is defined as

$$V(r, r + \Delta r, \Theta, \Theta + \Delta\Theta) = \frac{2}{3}\pi((r + \Delta r)^3 - r^3)$$
$$(\cos(\Theta) - \cos(\Theta + \Delta\Theta)) \quad (3)$$

The function $g_{A-B,C}(r, \Theta)$ can be represented in a 3D plot from which important angle relations can be derived. To allow the evaluation of the conventional RDF $g(r)$, the program has been modified such that specific angular areas can be selected. The new function $g_{A-B,C,\Theta_S,\Theta_R}(r)$ is based on the distribution function defined in eq 1 and can be written as

$$g_{A-B,C,\Theta_S,\Theta_R}(r) = \frac{1}{\Theta_R}\sum_{\Theta=\Theta_S}^{\Theta_S+\Theta_R} g_{A-B,C}(r, \Theta) \quad (4)$$

The coefficients Θ_S and Θ_R correspond to the start and the range of the angular area, respectively. Thus, by means of integration of this function over r, it is possible to determine the coordination number[28] of any given particle directly. This enables us to give quantitative information about local particle−particle interactions.

To describe directional correlations, we introduce the function $g_{A-B,C-D}(r, \Theta)$. Its definition is analogous to that of the function $g_{A-B,C}(r, \Theta)$ in eq 1 but with the vector $\mathbf{r}_{ik}$ replaced by the vector $\mathbf{r}_{kn}$, as shown in Figure 2. The function gives information about the number density of the directional correlations and the distances between the molecules.

To obtain the 3D spherical distribution of the correlated atom D around any molecule containing the atoms A, B, and C, we use the function $g_{A-B-C,D}(r)$. Here, the positions of A, B, and C define the *xy* plane of an internal coordinate system with the origin at the position of atom A. Typical 2D cuts of this function are shown in Figure 4a−c. The following time-dependent pair distribution functions $g_{A-B}(r, t)$ and $g_{A-B,C,r_S,r_R}(\Theta, t)$ are useful aids in determining the stability of clusters in the system. For the first function, the interatomic distances between atom A, the center of the correlation, and atoms B, which belong to the correlated (different) molecule are determined for any time interval $[t, t + \Delta t]$ within the total simulation time.

$$g_{A-B}(r, t) = \frac{V_{box}}{N_A N_B V(r, r + \Delta r)}$$
$$\sum_{\tau=t}^{t+\Delta t}\sum_{i=1}^{N_A}\sum_{k=1}^{N_B}\delta_{\Delta r}(r - |\mathbf{r}_{ik}(\tau)|) \quad (5)$$

Similarly, the function $g_{A-B,C,r_S,r_R}(\Theta, t)$ can be defined on the basis of $g_{A-B,C-D}(r, \Theta)$ but with the τ sum restricted to the interval $(t, t + \Delta t)$ and $\mathbf{r}_{ik}$ restricted to $r_S \le \mathbf{r}_{ik} \le r_S + r_R$. This function is standardized as $g_{A-B,C,r_S,r_R}(\Theta, t) \to 1$ for the radius interval $r_R \to \infty$. These functions can also be represented in a 3D plot (e.g., see Figure 16b).

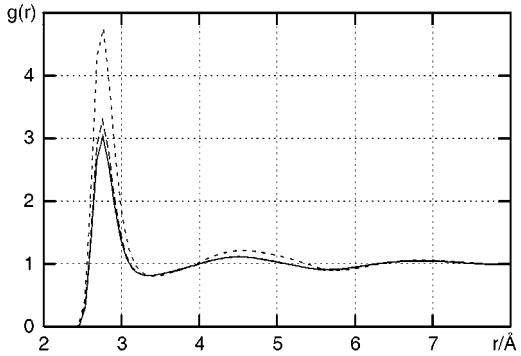

Figure 3. RDF $g_{O-O}(r)$ of the water component with 0 mol % AN (—), 2.2 mol % AN (− − −), and 24.8 mol % AN (· · ·).

Results and Discussion

First, we will investigate the structure of the AN cluster by means of the methods of analysis introduced above. Subsequently, we will focus on systems with low AN mole fractions in relation to their cluster tendency.

Structural Information. Water−Water. Figure 3 shows the pair correlation of oxygen−oxygen RDFs $g_{O-O}(r)$ of the water component in these mixtures. The peak heights at 2.8 Å increase with increasing AN concentration. With low mole fractions of AN (up to 4.7 mol %), the RDF is hardly distinguishable from that of pure water. The peaks are relatively low compared to the peaks of higher AN concentrations because of the nearly homogeneous distribution of the water molecules within the mixture: at low AN concentrations, more water molecules can be found in the far range of the simulation box than at higher concentrations, so statistical standardization ($g(r) \to 1$ as $r \to \infty$) leads to lower peaks in general and thus indicates a higher homogeneity of the mixture. In the distribution functions, there are also two lower maxima that represent additional hydration shells in the regions around 4.5 and 7.5 Å. Both the pronounced maximum and the short oxygen−oxygen distance of 2.8 Å between neighboring water molecules indicate strong interactions between the water molecules, which can be interpreted as hydrogen bonds. This interpretation is also confirmed by the RDFs $g_{O-H}(r)$, with the first peaks at 1.8 Å (not shown here). Figure 4a−c shows the coordination of the water's hydrogen (red) and oxygen atoms (blue) around the central water molecule. The central water molecule has been placed in the *xy* plane with the oxygen atom at the origin. This Figure clearly demonstrates the preferred orientation of the surrounding water molecules with respect to the central molecule. The hydrogen atoms are directed toward the oxygen of the central molecule, whereas the oxygen atoms are directed toward the hydrogen. The nonspherical water subshells can be seen in Figure 4c, where the water component becomes more structured. Thus, the microheterogeneity is built up.

Acetonitrile−Acetonitrile. When increasing the AN concentration, the peak heights of the first maxima become lower (see Figure 5), and the peaks are shifted toward larger atomic distances, from 3.6 to 4.2 Å. This decrease of the peak heights can be explained through the distribution of the molecules in the system as described in the preceding section. The increase of the AN concentration leads to larger nitrogen−nitrogen distances. The shifted peaks indicate a change in the cluster structure (see Figure 5). The same behavior has been reported by Kovacs and Laaksonen,[6,7] who used the standardized RDF.

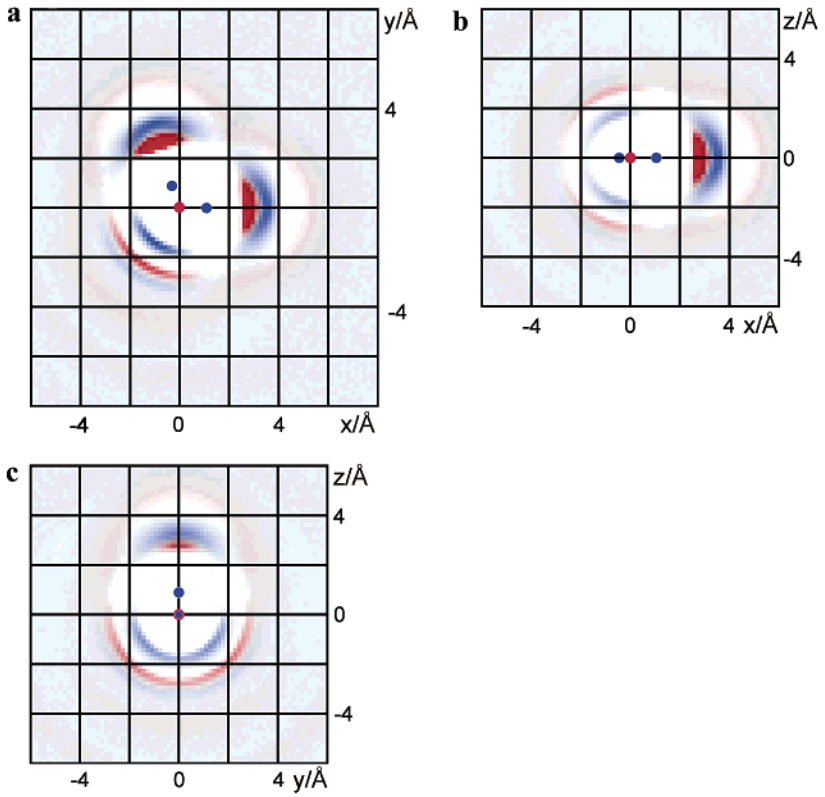

Figure 4. (a) Water surrounding a central water molecule (for 11.6 mol % AN; *xy* plane). (b) Water surrounding a central water molecule (for 11.6 mol % AN; *xz* plane). **(**c) Water surrounding a central water molecule (for 11.6 mol % AN; *yz* plane)

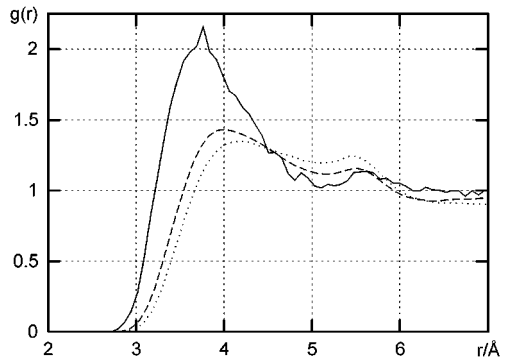

Figure 5. RDF $g_{N-N}(r)$ of the AN component with 2.2 mol % AN (—), 50 mol % AN (− − −), and 100 mol % AN (• • •).

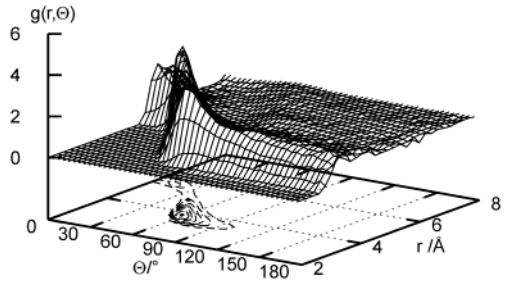

Figure 6. Angular-dependent RDF $g_{N-C(2),N}(r, \Theta)$ of the 11.6 mol % AN mixture. The correlated atom pairs are the nitrogen atoms of the AN molecules. The contour lines display the angular and radial positions of the local maxima.

An unexpected result was found for an AN concentration of 1.0 mol %. The peak height of the first maximum is just 1.3, which is less than that for neighboring concentrations of 0.5 and 1.6 mol %. This finding will be discussed below on the basis of the time-dependent RDF and angular distribution function.

The surroundings of a molecule in a microstructured system contain areas with few correlated atoms, so-called "structure holes". In the ideal case, these areas are represented by a local minimum with $g(r) < 1$ in the RDF, which follows a maximum with $g(r) > 1$, such as in the functions $g_{O-O}(r)$ in Figure 3. In other words, when the RDF shows a maximum followed by a minimum with $g(r) < 1$, one can conclude that this liquid is a microstructured system. However, an analysis of any such system does not necessarily result in a conventional RDF with a pronounced maximum and minimum. Because of the averaging over the whole angular range, the information on such extrema may disappear; it is, however, still present in the angular-dependent RDFs of these systems. Because they are restricted to certain angular intervals, the conventional RDFs may confirm the existence of minima, thus proving the existence of microstructure that is due to particular pairs of particles.

The current conventional RDFs, $g_{N-N}(r)$ in Figure 5, do not show any minima but do show a maximum within 3.6 and 4.2 Å, which is dependent on the concentration, and a shoulder near 5.5 Å.

The angular resolved view of these pair correlations, $g_{N-C(2),N}(r, \Theta)$ (see Figure 6), reveals that the shoulder in Figure 5 results from the superposition of a maximum over the angular range of $0° \leq \Theta \leq 40°$ and a minimum over $40° \leq \Theta \leq 90°$, which is behind the pronounced maximum (see Figure 6). Thus, this function, as in Figure 6, proves that the AN molecules of the mixture are arranged in a structured formation. The first maximum of the $g(r, \Theta)$ functions increases from 2.5 to 5.2 with $0° \leq \Theta \leq 60°$. This region represents the first shell of nitrogen atoms around the AN molecule. Over the range $60° < \Theta < 90°$ for $g(r, \Theta)$, the maximum decreases rapidly, and for $\Theta > 90°$, we have $1.5 < g(r, \Theta) < 2$. Consequently, in this region, the distribution of nitrogen atoms is lower, so we can

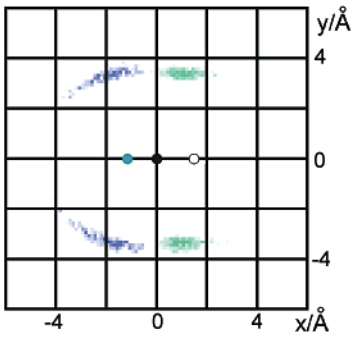

Figure 7. Surroundings of the AN molecule. The green area represents the distribution of nitrogen atoms, and the blue area, the methyl carbon atoms (green point: nitrogen, black: nitrile carbon, and white: methyl carbon atom).

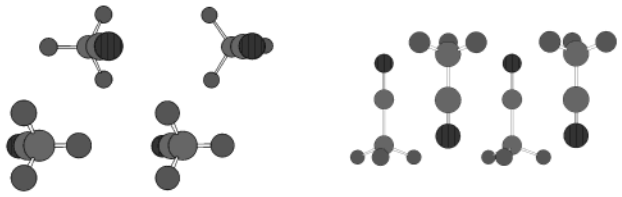

Figure 8. Sketches of the AN cluster structure. The left one illustrates the zigzag shape, and the right one, the antiparallel arrangement.

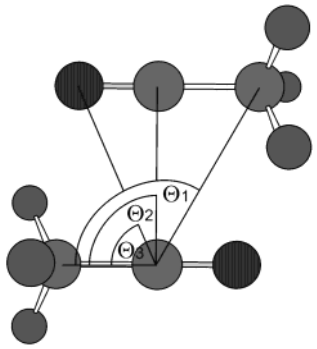

Figure 9. Definition of the angles θ_1, θ_2, and θ_3.

TABLE 2: Local Maxima of the Correlated Atoms C(2), C(1), and N with Respect to the Nitrile Carbon Atom C(1)

x^a/mol %	C(2), r/Å	θ_1/°	C(1), r/Å	θ_2/°	N, r/Å	θ_3/°
2.2	3.72	119	3.65	93	3.35	81
4.7	3.68	115	3.45	90	3.30	79
11.6	3.70	115	3.45	90	3.45	72
24.8	3.61	121	3.45	88	3.45	72
50.3	3.74	115	3.45	88	3.45	72
75.2	3.78	119	3.55	86	3.55	68
100	3.78	124	3.42	88	3.43	70

[a] Of AN.

conclude that the nitrogen atoms can be found mainly around the axis of the nitrile and methyl carbon atom, as shown in Figure 7. Figure 7 also shows that the bond axis between the nitrile carbon and methyl carbon atom is surrounded by other nitrogen atoms. The nitrogen and methyl carbon atoms around AN molecules are distributed separately. In conceiving a connection between these different areas, one would qualitatively consider an antiparallel and a slightly shifted arrangement of AN molecules. The observation of the surrounding area of the nitrile carbon atom, which is close to the mass center of the AN molecule, is helpful in further determinations of the AN cluster structure, as shown in the following section. To prove the antiparallel arrangement at various concentrations and for more detailed determinations, we focus on the surrounding area of the nitrile carbon atom, which is close to the mass center of the AN molecule.

Takamuku et al.[12] investigated AN mixtures with 10−100 mol % AN by means of IR and X-ray diffraction. For the pure AN liquid, they pointed out that the first neighbors are almost antiparallel and slightly shifted in such a way that the inner-atomic distance between the nitrile carbon and the nitrogen of the next neighbor is 3.5 Å and the distance vector is approximately perpendicular to the main molecular axis. The ANs of the second shell are directed parallel to the main molecule and are 4.1 Å apart. The result is a zigzag-shaped arrangement of the molecules in the cluster (see Figure 8).

Table 2 gives the interatomic distances and angles of the AN atoms in the first shell in relation to the main molecule, as shown in Figure 9, which are derived from the local maxima of the angular-dependent RDFs. This Table contains results only for concentrations corresponding to at least eight AN molecules. The angles Θ_1, Θ_2, and Θ_3 are taken from contours of the 3D plots of the angular-dependent RDFs $g_{C1-C2,C2}(r, \Theta)$, $g_{C1-C2,C1}(r, \Theta)$, and $g_{C1-C2,N}(r, \Theta)$, respectively. (See Figure 10a−c, which is evaluated from the systems listed in Table 2.) Comparing these angles (see Table 2), one finds that the AN molecules of the first shell are orientated almost antiparallel (see Figure 8). This orientation can be confirmed by an analysis of the correlation function $g_{C(1)-C(2),C(1)C(2)}(r, \Theta)$ (see Figure 11). The maximum, which is located at 180° and about 3.45 Å, represents the first shell and is therefore very distinct. Furthermore, there is another weak maximum at 0° and 4.1 Å, which represents the second shell. The sharpness of the first peak that was mentioned is a result of the large number of possible combinations with direct neighbors. These results agree very well with the experimental results of Takamuku et al.[12]

Considering the width of the local maxima in Figure 10a−c, we observed that the maximum of the angular-dependent RDF $g_{C1-C2,N}(r, \Theta)$ (Figure 10c) is quite sharp, whereas the signals in the functions $g_{C1-C2,C1}(r, \Theta)$ (Figure 10b) and $g_{C1-C2,C2}(r, \Theta)$ (Figure 10a) are relatively broad. This indicates that the molecules undergo librations, where the relative positions of the two nitrogen atoms are more or less fixed. Obviously, this effect depends on the AN concentration because with increasing AN concentration the peaks become more diffuse. The distance between neighboring nitrogen atoms increases significantly with increasing AN concentration (3.78−4.2 Å, see Figure 3), whereas the distance between the neighboring nitrile carbon atoms remains approximately the same (see Table 2). Obviously, the geometry of the cluster changes with increasing AN concentration. We assume that the AN molecules keep an antiparallel arrangement but tilt out at a point near the nitrile carbon atoms.

Acetonitrile−Water. To investigate the water molecules around an AN molecule, an angular-dependent RDF $g_{N-C(2),H(Wat)}(r, \Theta)$ (see Figure 12) is required. In the 3D plots for the various AN concentrations (e.g., in Figure 12 for a concentration of 11.6 mol %), one particular signal is very striking; this signal is very narrow and completely isolated in the angular region of $100° \leq \Theta \leq 180°$ and $r = 1.9$ Å. Moreover, the signal corresponds to the first sharp maximum at 1.9 Å in $g_{N-C(1),H(Wat),100°,80°}(r)$, which is shown in Figure 13. The peak heights increase with increasing AN concentration, and the peaks are followed by very pronounced minima, which are shifted with increasing AN concentration from 2.5 to 2.75 Å (see Figure 13). These distinctive extrema in the RDFs indicate strong electrostatic interactions between the water molecules and the AN molecules, which in this case can be interpreted as hydrogen

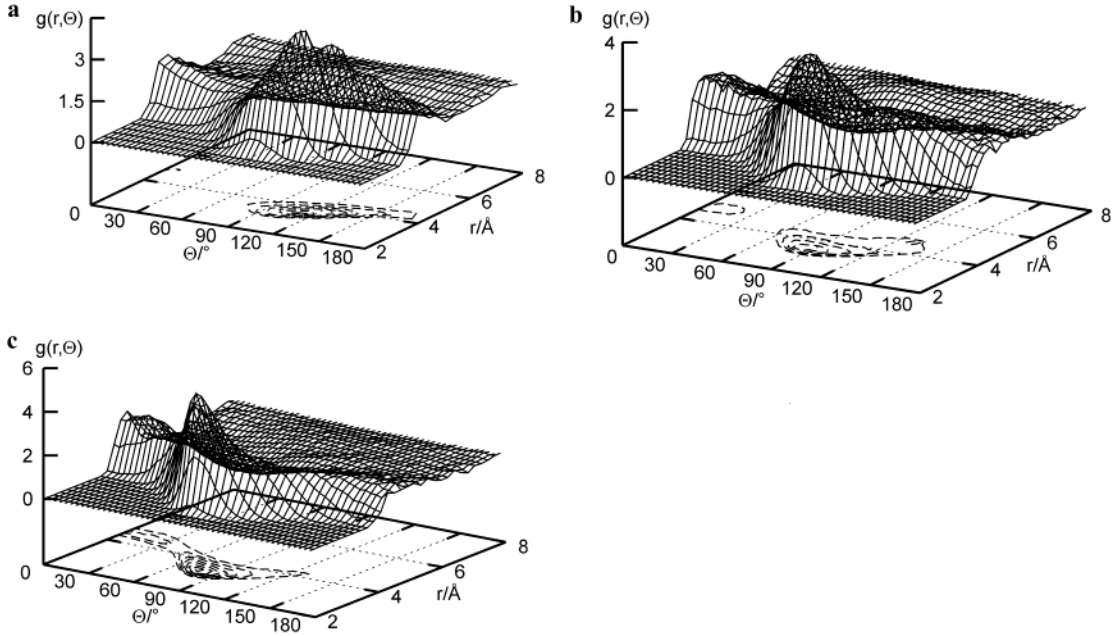

Figure 10. (a) Angle-dependent RDF $g_{C(1)-C(2),C(2)}(r)$ of the 11.6 mol % AN mixture. The correlated atom pairs are the nitrile carbon atom and the methyl carbon atom. (b) Angle-dependent RDF $g_{C(1)-C(2),C(1)}(r)$ of the 11.6 mol % AN mixture. The correlated atom pairs are the nitrile carbon atoms. (c) Angle-dependent RDF $g_{C(1)-C(2),N}(r)$ of the 11.6 mol % AN mixture. The correlated atom pairs are the nitrile carbon and nitrogen atom.

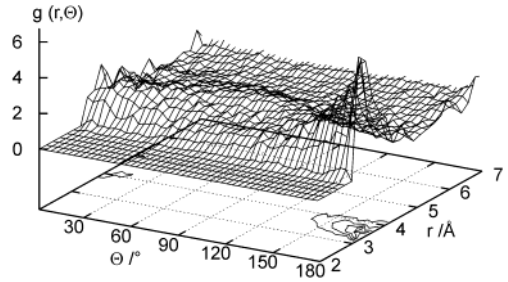

Figure 11. Exemplary angle-dependent RDF $g_{C(1)-C(2),C(1)-C(2)}(r)$ of the 11.6 mol % AN mixture.

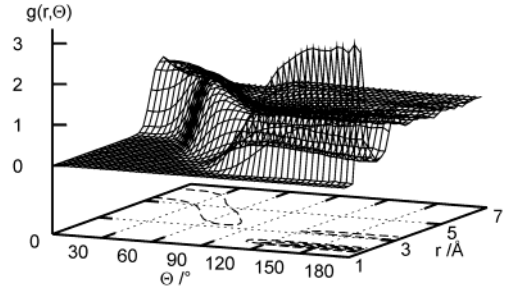

Figure 12. Angle-dependent RDF $g_{N-C(2),H(Wat)}(r, \Theta)$ of the 11.6 mol % AN mixture.

bonds. To obtain the coordination number of the hydrogen atoms at the nitrogen atoms, the integrals of the function $g_{N-C(2),H(Wat),100°,80°}(r)$ are evaluated to the first minimum. The coordination numbers as a function of the AN concentration are shown in Table 3. For example, we obtain for the 11.6 mol % system a coordination number of 3.23. Kovacs and Laaksonen[6,7] obtained a coordination number of 1, which is due to the fact that these authors evaluated only the integrals of the conventional functions $g_{N-H(Wat)}(r)$ without considering the specific angular range. These functions lead to a misleading number density of 1.5 at 1.9 Å because they result from averaging the number density over all angles. The lone electron pair at the nitrogen atom is able to form only one hydrogen bond. Thus, the high coordination number of 3.23 seems to be

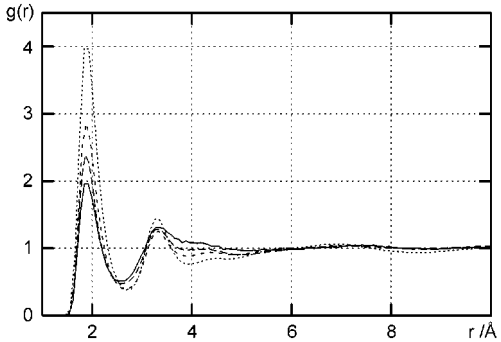

Figure 13. Distribution function $g_{N-C(1),H(Wat),100°,80°}(r)$ with AN concentrations of 0.26 mol % (—), 11.6 mol % (− − −) 50.3 mol % (- - -), and 75.2 mol % (• • •).

TABLE 3: Coordination Numbers of Water Oxygen and Hydrogen Atoms at the Methyl Carbon and the Nitrogen Atom of AN

x/mol % AN	C(2)−O	N−O	N−H	C(1)−C(1)*b*
0.26	18.54	9.45	3.71	
0.5	20.27	7.67	3.87	
1.0	18.89	9.83	3.73	
1.6	19.41	9.30	4.00	0.569
2.2	19.67	7.66	3.76	0.717
4.7	17.91	7.25	3.52	1.556
11.6	14.12	5.64	3.23	3.524
24.8	10.62	3.25	2.65	5.953
50.3	5.31	1.83	1.61	8.363
75.2	2.07	0.82	0.72	9.805
100	0	0	0	10.608

[a] Of AN. [b] Coordination numbers of the AN−AN cluster.

a contradiction. We assume the three hydrogen atoms can be bound alternately to the nitrogen atom via a hydrogen bond, but the other hydrogen atoms remain in the radial interval from 0 to 2.75 Å. Additionally, a former investigation of Luzar and Chandler[29] shows that a hydrogen bond requires specific geometric conditions that do not necessarily apply to each of the three hydrogen atoms simultaneously. Furthermore, when the mixture is at a low concentration, the coordination number

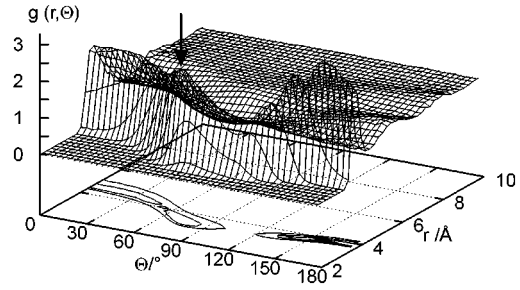

Figure 14. Angle-dependent RDF $g_{C(1)-C(2),O(Wat)}(r, \Theta)$ of the 11.6 mol % AN mixture. The arrow points to a local maximum, which disappears in the $g_{C(1)-C(2),O(Wat)}(r, \Theta)$ of mixtures of higher AN concentration.

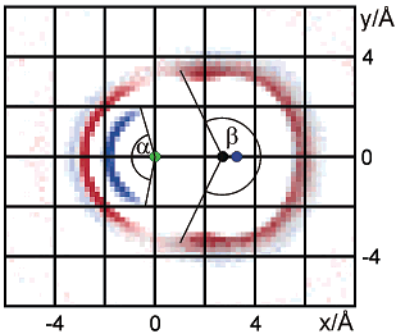

Figure 15. Local structure of hydrogen (blue) and oxygen (red) atoms surrounding the AN molecule of the AN/water system. On the nitrogen side (green point), there are distinguishable areas of hydrogen and oxygen atoms with an angular range of $\alpha = 160°$. On the methyl side, no explicit orientation of water molecules is visible. Only the water density is increased in the range of $\beta = 240°$. A gap of low density divides both areas.

of the oxygen atoms in the first shell is significantly higher (5.64 oxygen atoms vs 3.23 hydrogen atoms for the 11.6 mol % mixture) than the coordination number of the hydrogen atoms. This indicates that in the first shell most of the water molecules do not interact electrostatically with the nitrogen atom. However, with increasing AN concentration of the mixture, the coordination numbers of the oxygen and hydrogen atoms assimilate. For AN concentrations of more than 50 mol %, the water molecules seem to be bound to the nitrogen exclusively via hydrogen bonds. Another interesting detail is the weak local maximum in the angular-dependent functions $g_{C2-C1,O(Wat)}(r, \Theta)$ at $r = 3.45$ Å and $\Theta = 70°$ for low AN concentrations up to 11.6 mol % (see Figure 14 arrow), indicating a high local water density near the nitrile carbon atom of the nitrile group. At higher AN concentrations, the local maximum disappears as water is displaced, so we assume that the higher water oxygen atom density at low AN concentrations results from a weak dipole−dipole interaction between the AN molecules near the nitrile carbon atom and water molecules. In all probability, as in the model proposed by von Kabisch[3], at low AN concentrations, the AN molecules occupy free "cages" in the liquid water structure. In general, the coordination number of the oxygen atoms on the methyl side is higher than that on the nitrogen side of the AN molecules (see Table 3, C−O vs N−O). Figure 15 shows the preferred orientation of the water molecules on the nitrogen side of the AN molecules, but this orientation is not due to the lack of electrostatic interactions on the methyl side, as expected. The relatively high coordination number and the unarranged orientation at the methyl side hint that this group dominantly effects a displacement of the water molecules in the solution.

Cluster Properties of the AN/Water Systems. To investigate the cluster properties of the AN/water systems, we have analyzed the time-dependent RDF. For concentrations of $c < 2.2$ mol %, the distances between two nitrile carbon atoms vary in time, indicating Brownian motion. At a concentration of $c = 2.2$ mol %, the distances are constant over a long time interval, but the relative orientation of two molecules with a distance of $3.0 \leq r \leq 4.5$ Å is not constant. Therefore, one can conclude that the AN cluster with anti and parallel arrangements does not occur permanently (see Figure 16a,b). For concentrations of $c \geq 4.7$ mol %, both the distances and orientation are conserved over a long time interval, which is a result of the formation of AN clusters with the "correct" arrangement. Figure 17a,b shows the ideal case, that of a constant distance between neighboring

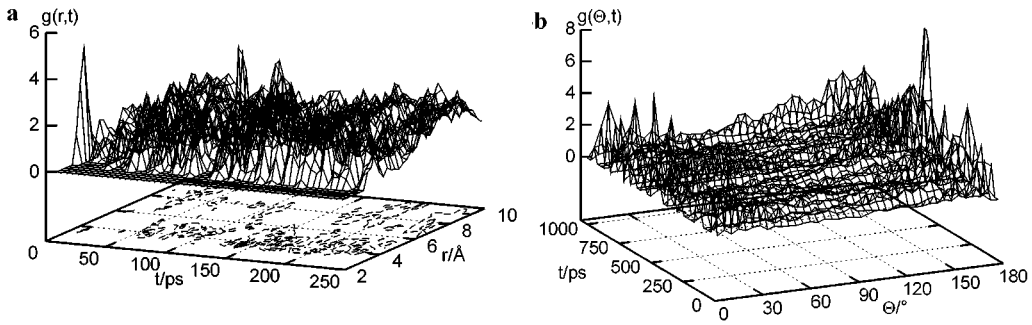

Figure 16. (a) $g_{C(1)-C(2),C(1)-C(2)}(r, t)$ of the 2.2 mol % AN mixture. (b) $g_{C(1)-C(2),C(1)-C(2),3.0\ Å,1.5\ Å}(\Theta, t)$.

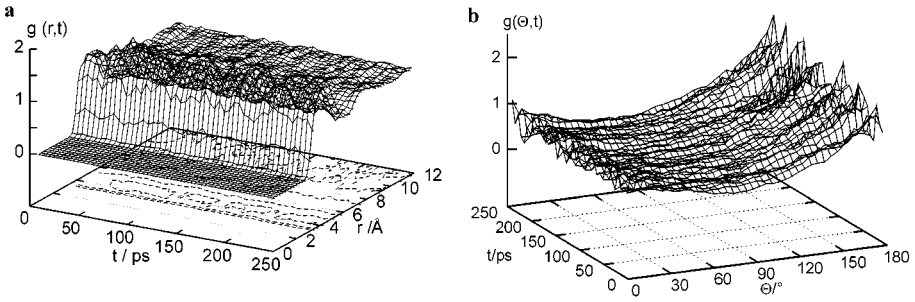

Figure 17. (a) $g_{C(1)-C(2),C(1)-C(2)}(r, t)$ of the 25 mol % AN mixture. (b) $g_{C(1)-C(2),C(1)-C(2),3.0\ Å,1.5\ Å}(\Theta, t)$.

molecules (see Figure 17a) and a preferred orientation of $\Theta = 180°$ for $r \approx 3.5$ Å and $\Theta = 0°$ for $r \approx 4.0$ Å (see Figure 17b).

Conclusions

We have carried out molecular dynamics simulations of liquid water, acetonitrile (AN), and AN/water mixtures. Within an AN concentration range of 0.26−75.2 mol %, the local structure of bulk water does not change significantly. However, the corresponding RDFs indicate increasing inhomogeneity with increasing AN concentration, which confirms the existence of interactions between AN molecules and water molecules.

For pure liquid AN, Kratochwill et al.[30] proposed, on the basis of their X-ray diffraction experiments, a model of an AN cluster. The crystallographic orthorhombic unit cell with a volume of 694 Å^3 contains eight AN molecules. Furthermore, these authors assumed an alternately antiparallel and parallel arrangement of the molecules. Bertagnolli et al.[31] proved by X-ray and neutron-ray diffraction that the dipole−dipole interactions at short distances are essential and that the direction of the molecules is preferably antiparallel. In our corresponding simulation, the cubic simulation box of the pure AN system contains 320 molecules, and the length of its edge is 30.354 Å. Thus, the volume of a subbox containing eight AN molecules is 699.178 Å^3, in agreement with experiment. The antiparallel arrangement of the molecules, which is found from the analysis of the various angular-dependent distribution functions, and the dimensions of the subbox confirm the models of Bertagnolli.[31]

Our simulations also confirm the dominant factors for clustering, as suggested by Kratochwill,[30] namely, the space occupation of the AN molecules and the dipole−dipole interactions. The space occupation requirements force the molecules to form local surroundings such that the distance between neighboring ANs is 3.45 Å. The dipole−dipole interaction effects the antiparallel arrangement of the molecules. The smallest AN fraction for permanent AN clustering can be found at an AN concentration of 4.7 mol % at 300 K.

The local water structure around the AN molecule is itself heterogeneous; the corresponding angular-dependent RDFs show that the hydrogen atoms of the water molecules are clearly arranged toward the nitrogen atom. Furthermore, the pronounced shape of the functions indicates that this arrangement is induced by strong electrostatic interactions that can be interpreted as hydrogen bonds. However, the coordination number near the methyl carbon atom is relatively high, but there is no preferred arrangement of the water molecules toward the methyl side because the water molecules are displaced by the methyl groups. The typically macroscopic properties of AN/water mixtures can be attributed to microscopic behavior: H-bonds and strong electrostatic interactions between the water and AN molecules lead to a macroscopically homogeneous solution over a wide mole and temperature range. The density of the macroscopic fluid depends on the mole fraction of the solution. Cunningham et al.[32] found that the density decreases parabolicly with increasing AN fraction from 0.997 to 0.777 g cm^{-3} at 298 K. The displacement of water molecules by the AN's methyl groups leads to a fast decay of the density at low AN mole fractions, which is in line with the coordination number of water oxygen atoms on the methyl side (see Table 3). The spherical distribution of the water molecules around the methyl group is determined by the cage formed by the AN molecules, depending on the AN concentration. To obtain the detailed information on the liquid structure presented in this work, it was necessary to go beyond the conventional pair correlation functions.

Acknowledgment. We thank Professor J. Hinze for helpful suggestions and support and T. Scott for revision of this text. This work was financially supported by the Project Molekül Dynamik (OZ. 21442) of the Deutsche Forschungsgemeinschaft (DFG). We gratefully acknowledge the computer resources made available to us by the computer center (HRZ) of the Universität Bielefeld.

References and Notes

(1) Robertson, R. E.; Sugamori, S. E. *Can. J. Chem.* **1972**, *50*, 1353.
(2) Moreau, C.; Douhéret, G. *J. Chim. Phys. Phys.-Chim. Biol.* **1974**, *71*, 1313. Moreau, C.; Douhéret, G. *Thermochim. Acta* **1975**, *13*, 385. Moreau, C.; Douhéret, G. *J. Chem. Thermodyn.* **1976**, *8*, 403. Moreau, C.; Douhéret, G.; Viallard, A. *Fluid Phase Equilib.* **1985**, *22*, 289. Moreau, C.; Douhéret, G.; Viallard, A. *Fluid Phase Equilib.* **1986**, *26*, 221.
(3) von Kabisch, G. *Z. Phys. Chem.* **1982**, *263*, 48.
(4) Naberukhin, Yu. I.; Rogov, V. A. *Russ. Chem. Rev.* **1971**, *40*, 207.
(5) v. Goldammer, E.; Hertz, H. G. *J. Phys. Chem.* **1970**, *74*, 3734.
(6) Kovacs, H.; Laaksonen, A. *J. Am. Chem. Soc.* **1991**, *113*, 5596.
(7) Bergman, D. L.; Laaksonen, *A. Phys. Rev. E* **1998**, *58*, 4706.
(8) Berendsen, H. J. C.; Postma, J. P. M.; van Gunsteren, W. F.; Hermans, J. *Intermolecular Forces*; Pullman, B., Ed.; Reidel: Dordrecht, The Netherlands, 1981.
(9) Böhm, H.; McDonald, I.; Madden, P. *Mol. Phys.* **1983**, *49*, 347.
(10) Mountain, R. D. *J. Chem. Phys.* **1999**, *103*, 10744.
(11) Berendsen, H. J. C.; Grigera, J. R.; Straatsma, T. P. *J. Phys. Chem.* **1987**, *91*, 6269.
(12) Takamuku, T.; Tabata, M.; Yamaguchi, A.; Nishimoto, J.; Kumamoto, M.; Wakita, H.; Yamaguchi, T. *J. Phys. Chem. B* **1998**, *102*, 8880.
(13) Toensing, T.; Oldiges, C. *Phys. Chem. Chem. Phys.* **2001**, *3*, 5542.
(14) Böhm, H. J.; Lynden-Bell, R. M.; Madden, P. A. *Mol. Phys.* **1983**, *49*, 349.
(15) Woodcock, L. V. *Chem. Phys. Lett.* **1971**, *10*, 257.
(16) Swope, W. C.; Andersen, H. C.; Berens, P. H.; Wilson, K. R. *J. Chem. Phys.* **1982**, *76*, 637.
(17) Andersen, H. C. *J. Comput. Phys.* **1983**, *52*, 24.
(18) Allen, M.; Tildesley, D. *Computer Simulation of Liquids*; Clarendon Press: Oxford, 1987.
(19) Berendsen, H. J. C.; Postma, J. P. M.; van Gunsteren, W. F.; DiNola, A.; Haak, J. R. *J. Chem. Phys.* **1984**, *81*, 3684.
(20) Jorgensen, W. L. *J. Am. Chem. Soc.* **1982**, *103*, 335.
(21) de Leeuw, S.; Perram, J.; Smith, E. *Proc. R. Soc. London, Ser. A* **1980**, *373*, 27.
(22) Heyes, D. *J. Chem. Phys.* **1981**, *74*, 1924.
(23) Smith, P.; Pettitt, B. *Comput. Phys. Commun.* **1995**, *91*, 339.
(24) Smith, P.; Pettitt, B. *J. Chem. Phys.* **1996**, *105*, 4289.
(25) Toukmaji, A. Y.; Board, J. A. *Comput. Phys. Commun.* **1996**, *95*, 73.
(26) Pollock, E.; Glosli, J. *Comput. Phys. Commun.* **1996**, *95*, 93.
(27) Haberlandt, R.; Fritzsche, S.; Peinel, G.; Heinzinger, K. *Molekulardynamik*; Vieweg: Braunschweig/Wiesbaden, 1995.
(28) Chandler, D. *Introduction to Modern Statistical Mechanics*; Oxford University Press: New York, 1987.
(29) Luzar, A.; Chandler, D. *J. Chem. Phys.* **1993**, *98*, 8160.
(30) Kratochwill, A.; Weidner, J. U.; Zimmermann, H. *Ber. Bunsen-Ges. Phys. Chem.* **1973**, *77*, 408.
(31) Bertagnolli, H.; Zeidler, M. D. *Mol. Phys.* **1978**, *35*, 177.
(32) Cunningham, G. P.; Vidulich, G. A.; Kay, R. L. *J. Chem. Eng. Data* **1967**, *12*, 336.